Supplementary Figures

A novel VRS5 isoform untangles pleiotropic effects on barley tillering and row-type

Ton Winkelmolen[1], Pierangela E. Colleoni[1], Marijke Hartog[1], Parastoo Hoseinzadeh[2], Ralf-Christian Schmidt[3], Richard G. H. Immink[1,4,5], and G. Wilma van Esse[1]*

[1]Laboratory of Molecular Biology, Wageningen University and Research, 6708 PB Wageningen, The Netherlands
[2]KWS SAAT SE & Co. KGaA, 37574 Einbeck, Germany
[3]BASF Belgium Coordination Center CommV, Technologiepark 101, 9052 Gent Zwijnaarde, Belgium
[4]Bioscience, Wageningen Plant Research, Wageningen University and Research, 6708 PB Wageningen, The Netherlands
[5]Current affiliation: Laboratory of Cell and Developmental Biology, Wageningen University and Research, 6708 PB Wageningen, The Netherlands

*Author for correspondence: wilma.vanesse@wur.nl

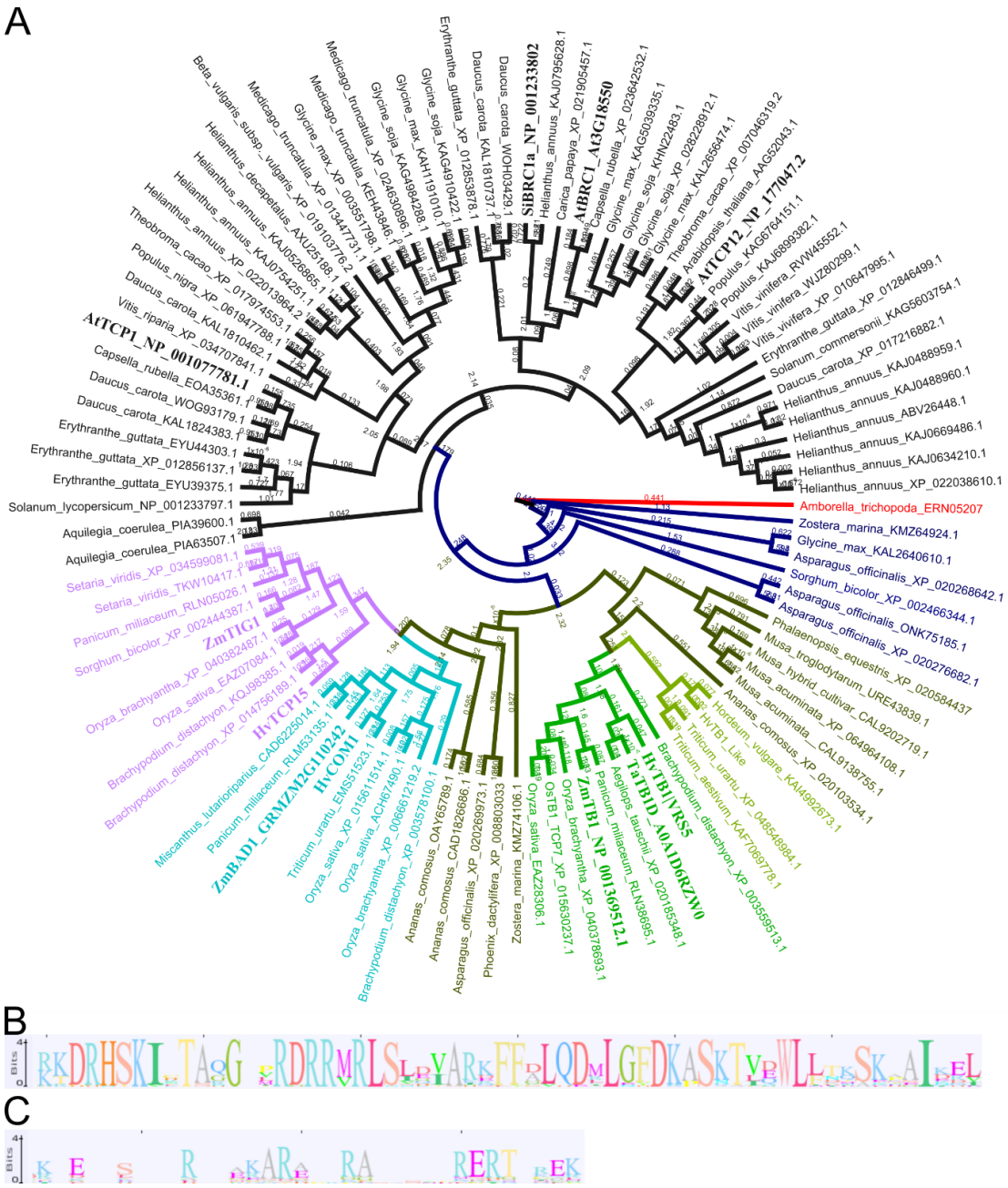

Figure S1: Phylogenetic analysis of TB1 and BRC1 in monocots and dicots. A) Phylogenetic analysis of TB1/BRC1. TB1 (green) and BRC1 (blue) homologs based on blastp of Maize, Barley, and wheat TB1 (ZmTB1, HvVRS5 (HvTB1), TaTB1D) as well as Arabidopsis and Tomato BRANCHED1 (AtBRC1, SlBRC1). This shows that divergence of the TB1 clade occurred after the monocot/dicot split. Amborella (red) was used as an outgroup. In black, dicot sequences clustering with BRC1, AtTCP1 and AtTCP12. Purple: sequences clustering with ZmTIG1 and HvTCP15, Cyan: sequences clustering with ZmBAD1 and HvCOM1, Green: Sequences clustering with VRS5, HvTB1, and OsTB1. Light green: *Triticeae*-specific duplication containing HvTB1-like. Brown: Other monocot TCPs diverged after the monocot dicot split. Dark blue, dicot and monocot TCPs that are not in the BRC1 or TB1 clades. Convergence was met after 400 bootstraps, based on a AutoMRE model. The tree was generated using RaXML and visualized in Geneious prime. B) Protein sequence consensus motif of the TCP-domain of all TCPs in the tree. C) Protein consensus motif of the R-domain of all TCPs in the tree.

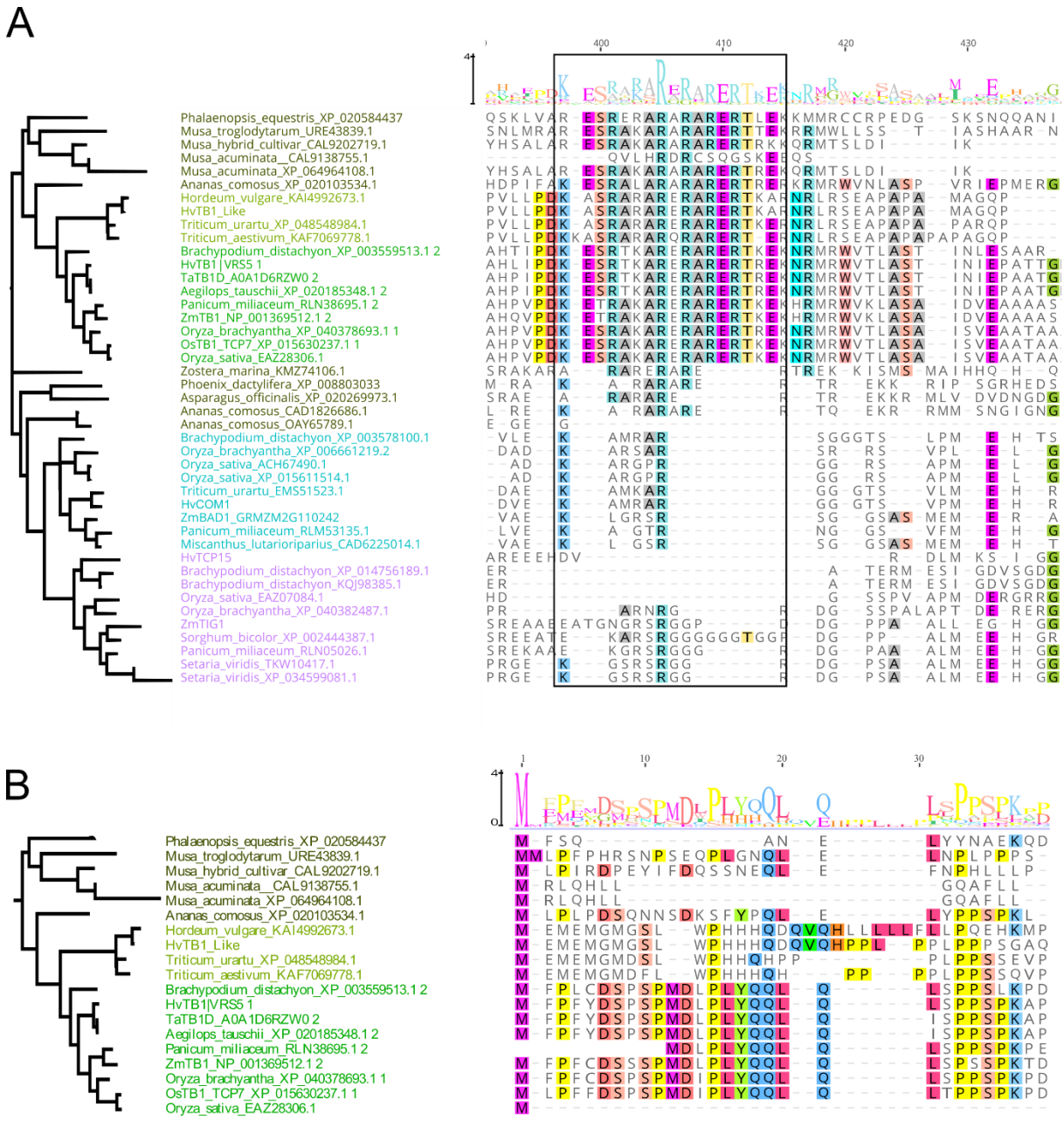

Figure S2: Conservation of the R-domain and SP-domain in monocot CYC/TB1 TCPs A) protein alignment of the R-domain of the grass-specific clade of CYC/TB1 TCPs. B) Protein alignment of the SP-domain, only present in the sub-clade containing VRS5, ZmTB1 and OsTB1.

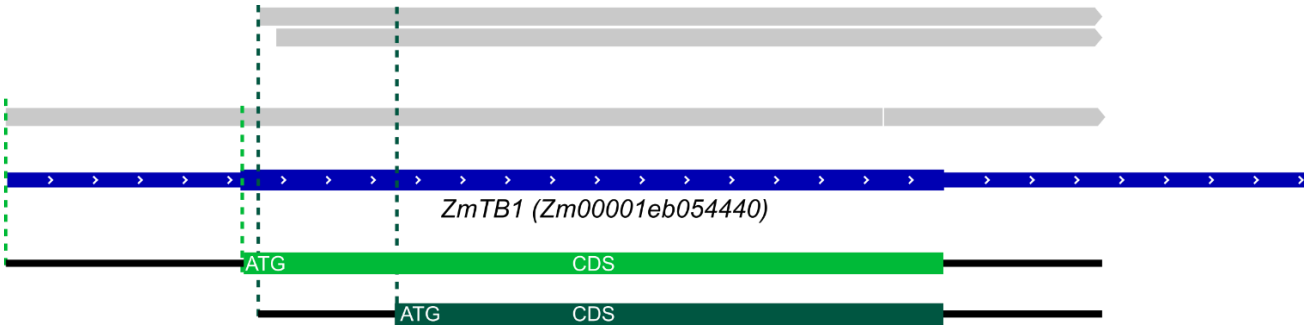

Figure S3: Long read sequencing of maize shows two TB1 isoforms. Long read RNA sequencing data of maize B73 (Wang et al., 2016) was re-analyzed and mapped against ZmTB1 from maize NAM5.0 (Hufford et al., 2021). The dashed green lines represent the location of the start codon and transcriptional start site (TSS) of ZmTB1α and ZmTB1β respectively, showing a schematic overview of the two *TB1* isoforms and their corresponding coding sequences (CDS).

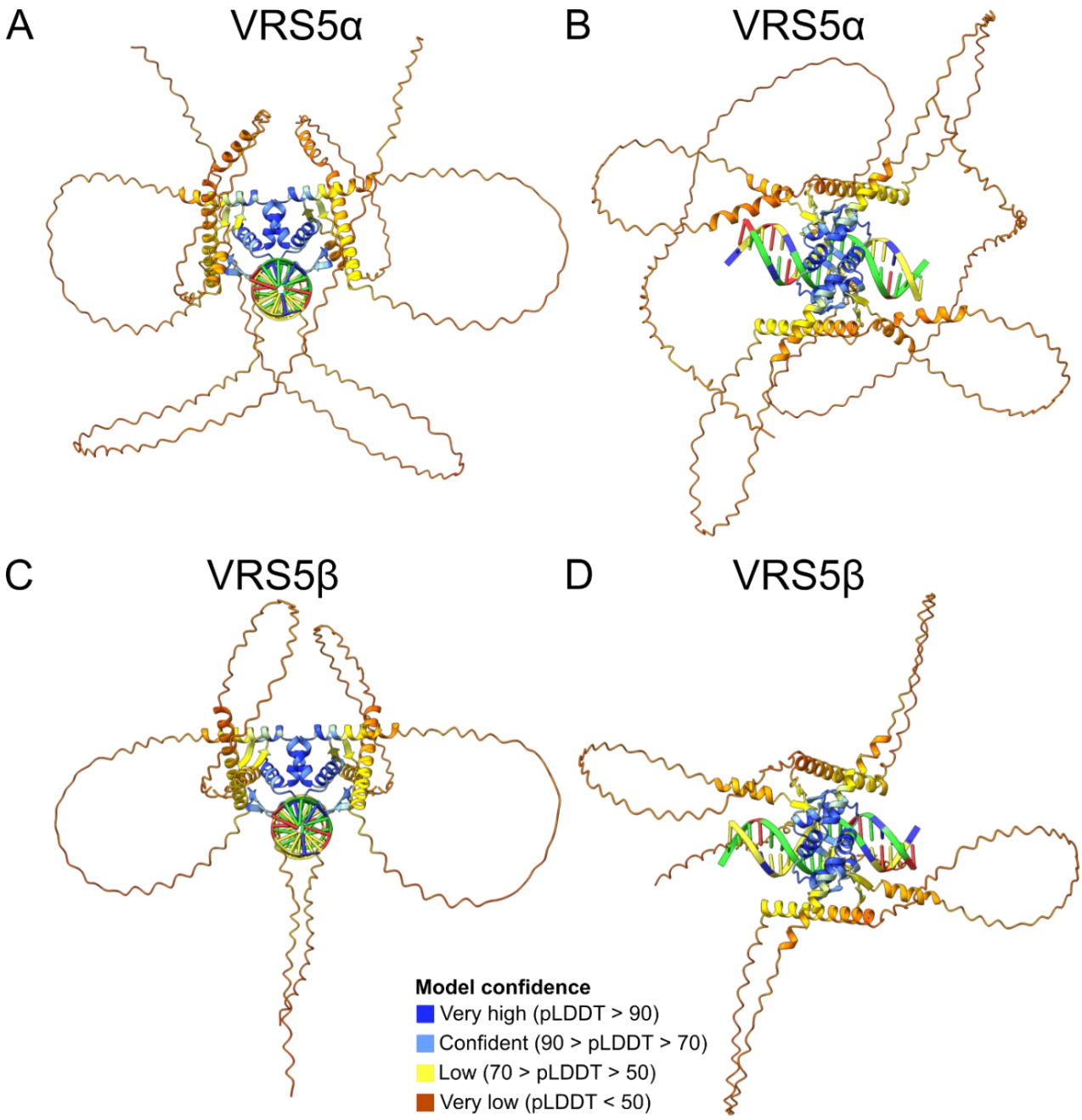

Figure S4: Alphafold-based predictions of the 3D structure of VRS5 isoforms. A+B) VRS5α heterodimer binding to DNA from the A) front and B) top and C+D) VRS5β heterodimer binding to DNA from the C) front and D) top. Color of the protein structure is based on the model confidence (pLDDT), showing that in both cases the TCP domain, forming several alpha helices coupled by small loops and binding the DNA is predicted confidently. Other parts of the proteins are predicted with low confidence.

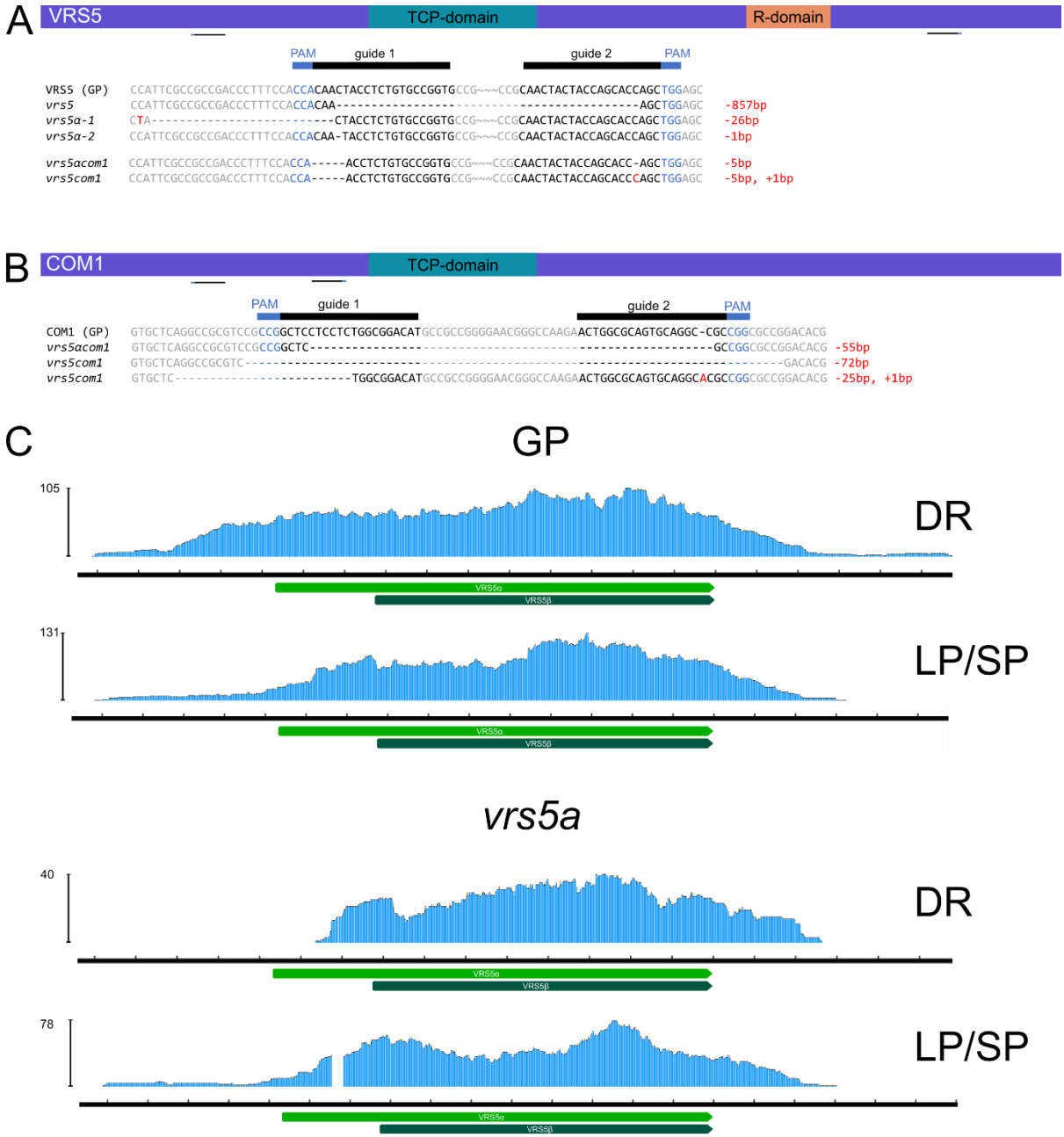

Figure S5: Mutations of created CRISPR mutants of A) VRS5 and B) COM1 C) RNA-Seq reads of the *vrs5α-1* line aligned to VRS5

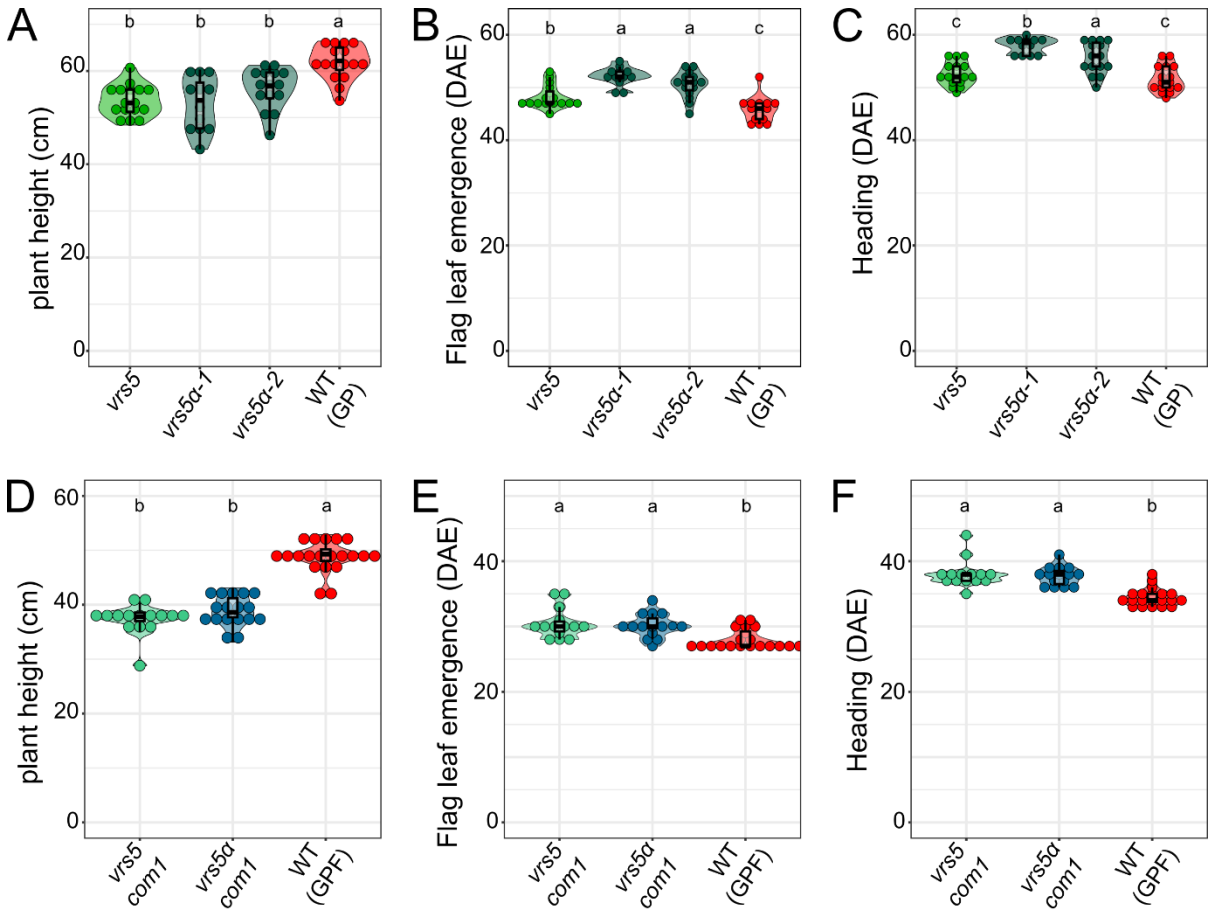

Figure S6: Plant height and flowering time of *vrs5* and *vrs5com1* double mutants. Plots of A) plant height, B) days to flag leaf emergence, and C) days to heading of *vrs5, vrs5α-1, vrs5α-2,* and WT (cv. Golden promise). Plots of D) plant height, E) days to flag leaf emergence, and F) days to heading of *vrs5com1, vrs5αcom1,* and WT (cv. Golden Promise Fast). Different letters indicate significant ($p < 0.05$) differences between the lines calculated using one-way ANOVA followed by Tukey's HSD (A) or Kruskal-Wallis test followed by Dunn's to adjust for multiple testing (B,C,D,E,F). $n \geq 12$ biological replicates.

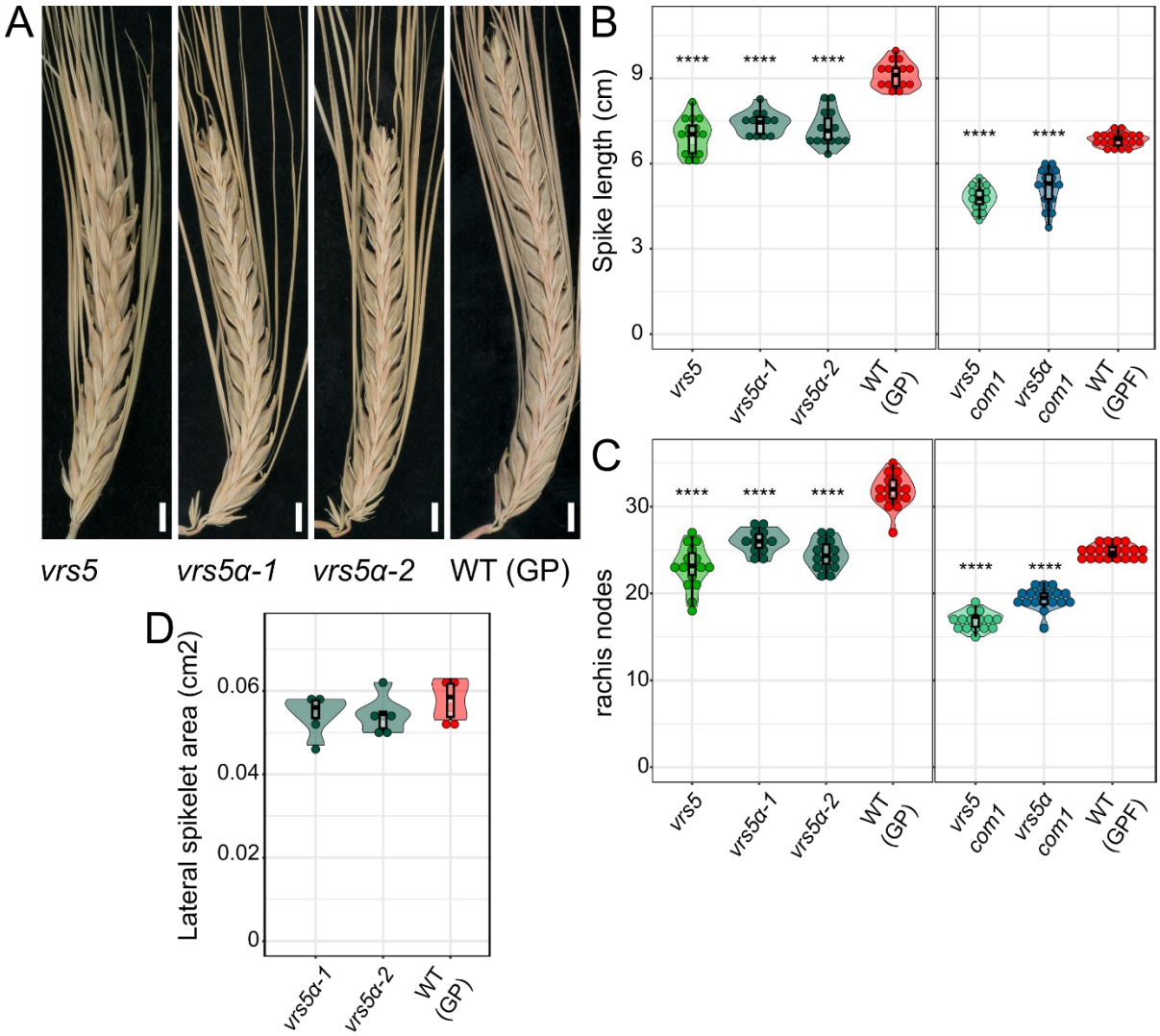

Figure S7: Detailed spike phenotype of vrs5 isoform mutants A) Spike images of *vrs5*, *vrs5α-1*, *vrs5α-2*, and wildtype (cv. Golden Promise). Plot of B) spike length and C) number of rachis nodes of *vrs5*, *vrs5α-1*, *vrs5α-2*, and wildtype (cv. Golden Promise); and *vrs5com1*, *vrs5αcom1*, and wildtype (cv. Golden Promise fast). n ≥ 12 biological replicates. D) Plot of average lateral spikelet area of ten non-developed sterile lateral spikelets of six plants of the two-rowed lines *vrs5α-1*, *vrs5α-2*, and wildtype (cv. Golden Promise). n = 6 biological replicates. Asterisks indicate statistical differences between the mutant lines and their respective wild type. (****: $p < 0.0001$), calculated using Kruskal-Wallis test followed by Dunn's to adjust for multiple testing.

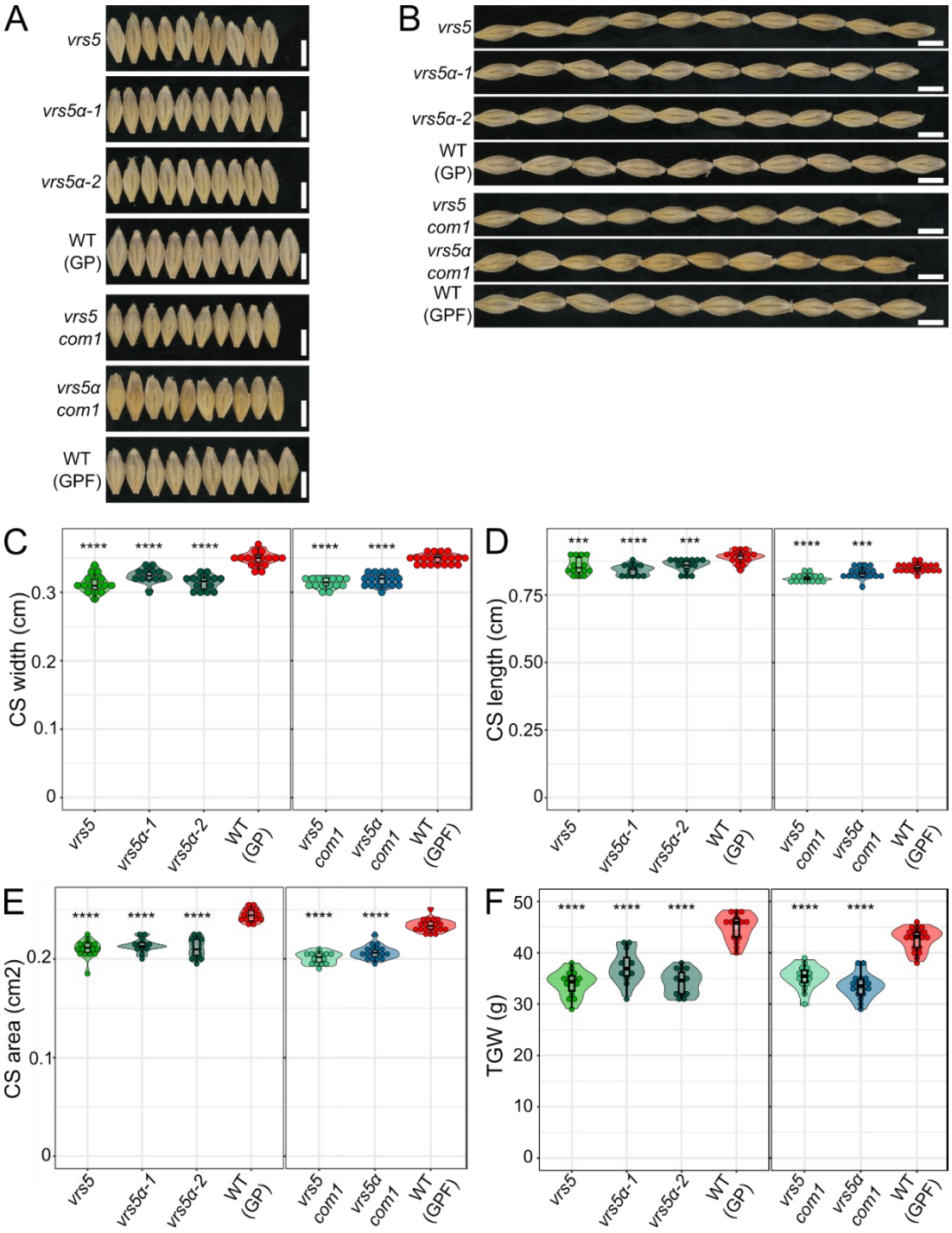

Figure S8: Detailed central spikelet phenotype of *vrs5* isoform mutants A+B) Pictures of ten central spikelets of *vrs5, vrs5α-1, vrs5α-2,* and wildtype (cv. Golden Promise); and *vrs5com1, vrs5αcom1,* and wildtype (cv. Golden Promise fast). Plots of central spikelet (CS) C) width, (D) length, (E) Area, and (F) thousand grain weight (TGW) of *vrs5, vrs5α-1, vrs5α-2,* and wildtype (cv. Golden Promise); and *vrs5com1, vrs5αcom1,* and wildtype (cv. Golden Promise fast). Asterisks indicate statistical differences between the mutant lines and their respective wild type. (***: $p < 0.001$, ****: $p < 0.0001$), calculated using D) Kruskal-Wallis test followed by Dunn's to adjust for multiple testing, or C,E,F) One-way ANOVA followed by Tukey's HSD to adjust for multiple testing. $n \geq 12$ biological replicates.

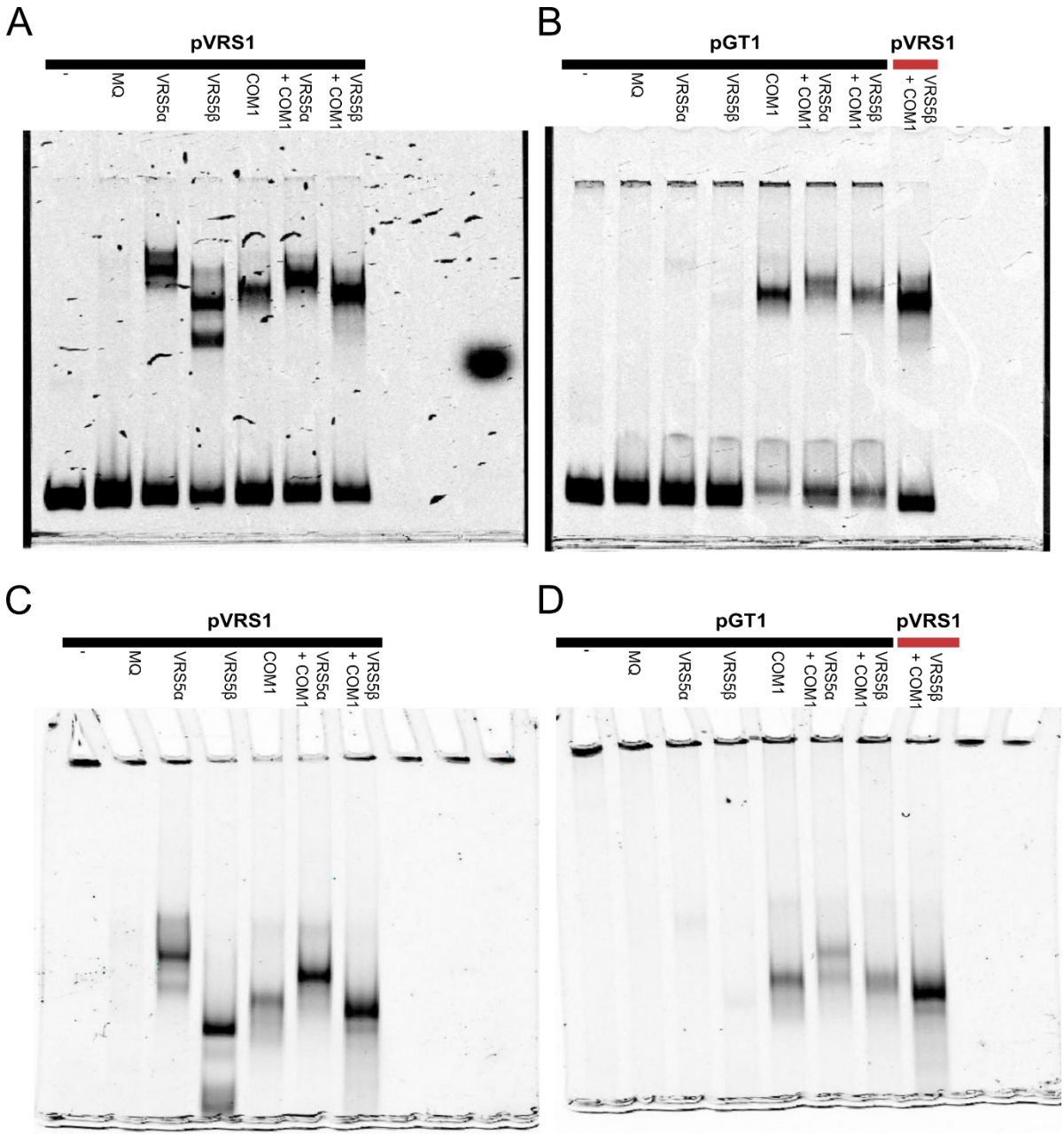

Figure S9: Full EMSA gels. Full EMSA gels of VRS5 isoforms and HvCOM1 binding to an infrared-labeled DNA probe in the A+C) *VRS1* promoter or B+D) *GT1* promoter after running for A+B) 1.5h and C+D) 3h.

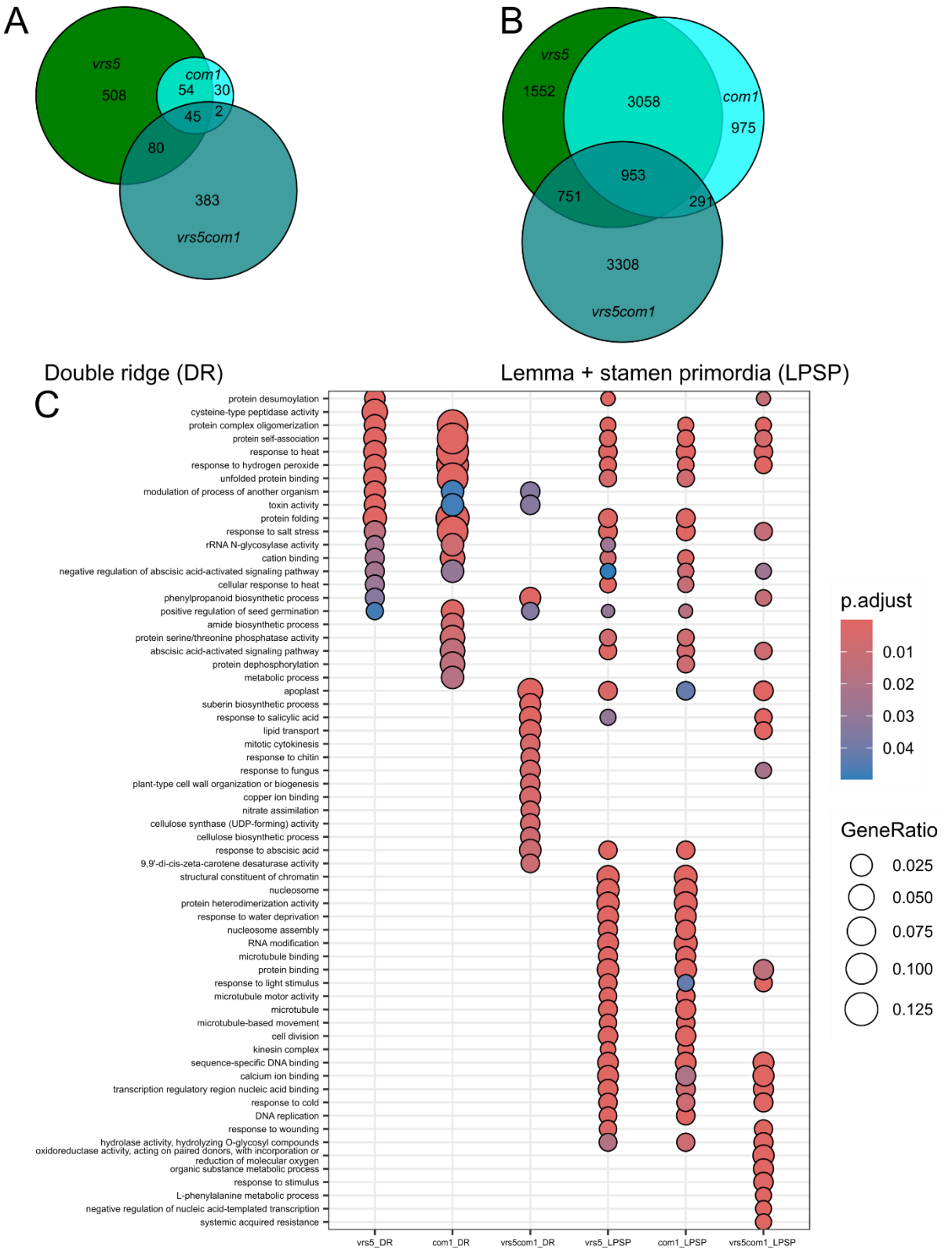

Figure S10: overlap in differentially expressed genes and GO-enrichment. Venn diagrams of overlap between differentially expressed genes (DEGs) in *vrs5, com1,* and *vrs5com1* compared to their respective wild-type (Golden Promise for *vrs5* and *com1,* Golden Promise Fast for *vrs5com1*) in developing inflorescences at A) double ridge (DR) and B) lemma and stamen primordia (LPSP) stage. C) Enriched GO-terms in DEGs for each comparison. Only the top 15 enriched GO-terms are shown, unless another GO-term is enriched and shared with another comparison.

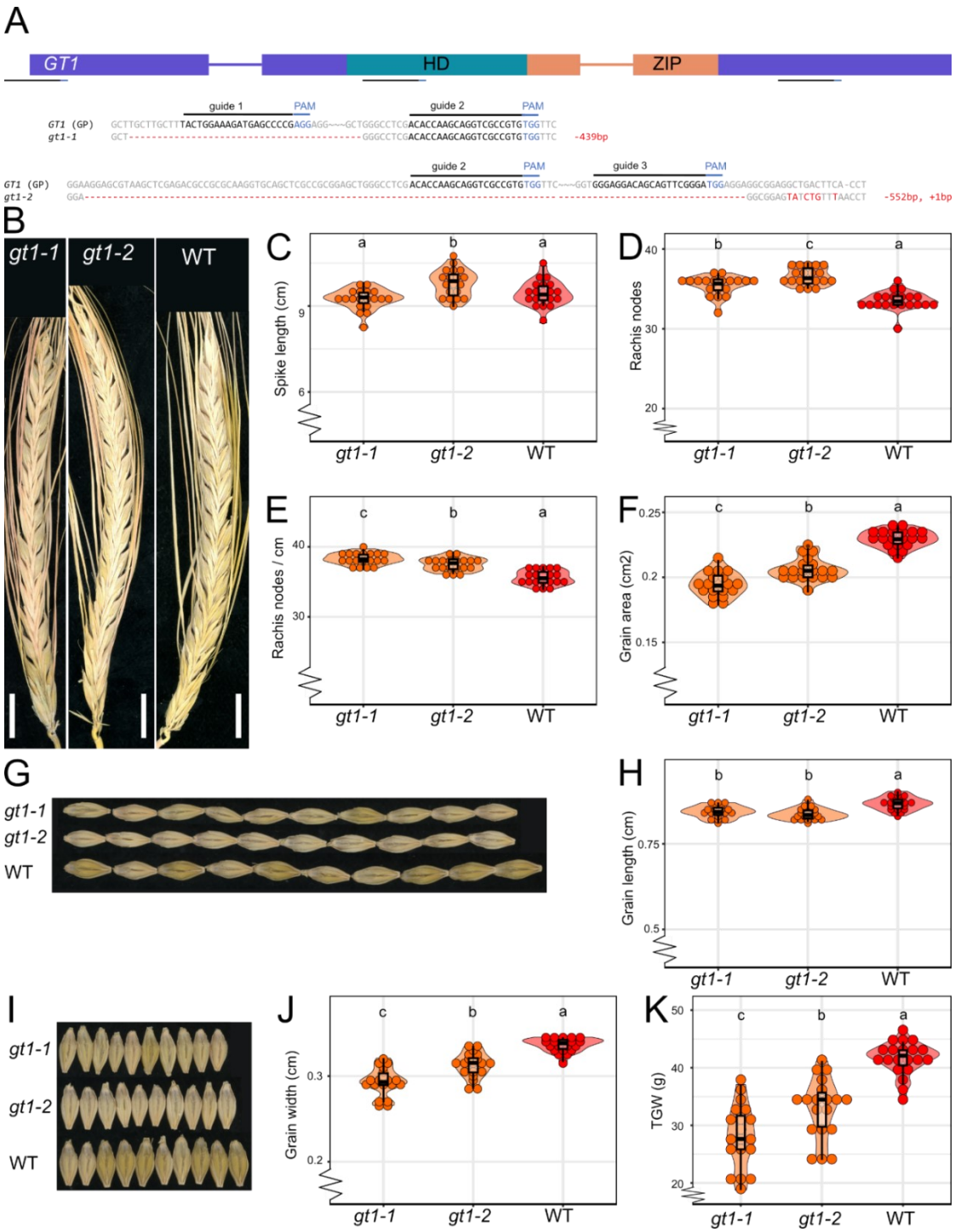

Figure S11: Spike phenotype of *HvGT1* mutants A) overview of created CRISPR mutants of *HvGT1*. B) representative spikes of *gt1-1, gt1-2, and* WT (cv. Golden Promise). Plots of C) spike length, D) number of rachis nodes, E) rachis nodes density, and F) grain area of *gt1-1, gt1-2, and* WT (cv. Golden Promise). G) Pictures of ten grains of *gt1-1, gt1-2, and* WT (cv. Golden Promise) as representation of grain length. H) plot of grain length of *gt1-1, gt1-2, and* WT (cv. Golden Promise). I) Pictures of ten grains of *gt1-1, gt1-2, and* WT (cv. Golden Promise) as representation of grain width. Plots of J) grain width and K) thousand grain weight (TGW) of *gt1-1, gt1-2, and* WT (cv. Golden Promise). Different letters indicate significant ($p < 0.05$) differences between the lines calculated using one-way ANOVA followed by Tukey's HSD (C, E, F, H) or Kruskal-Wallis test followed by Dunn's to adjust for multiple testing. $n \geq 19$ biological replicates.